ChemComm

COMMUNICATION

View Article Online
View Journal | View Issue

Cite this: *Chem. Commun.*, 2024, **60**, 5082

Received 22nd March 2024,
Accepted 13th April 2024

DOI: 10.1039/d4cc01313a

rsc.li/chemcomm

A high-performance chiral ^{19}F-labeled probe with an increased structural twisting†

Chenyang Wang,‡[ab] Guangxing Gu,‡[b] Wei Zhang,[b] Jian Wu[c] and Yanchuan Zhao *[abc]

We developed a new strategy to enhance the chiral discrimination capability of ^{19}F-labeled probes by tuning the torsion angle of the probe's backbone, allowing for the resolution of challenging analytes. Its versatility is demonstrated through the superior performance and the wide analyte scope.

Analytical techniques are crucial in various domains, providing precise data that forms the foundation for critical decisions in medical diagnosis, food quality assurance, and the detection of illegal substance use.[1] The growing demand for rapid and accurate detection methods continues to drive scientific research and technological advancements.[2] Among these, chiral discrimination has emerged as a key area of intense investigation.[3] The chirality of molecules significantly influences their biological and pharmaceutical properties, which is widely acknowledged in scientific communities.[4] Moreover, chirality plays a pivotal role in optical and self-assembling behaviours, contributing to the efficacy of advanced functional materials.[5] These distinctive properties and their broad applications underscore the significance of chirality and its related research. Nonetheless, the progression of chiral science is still limited by the lack of fast and precise analytical methods for analysing complex mixtures. Currently, the analysis of chiral compounds primarily relies on chromatographic techniques.[6] Despite their broad applicability, these methods often require pre-purification of the analytes, selection of a suitable stationary phase, and careful screening of the eluting conditions. Analytes with low UV absorption often necessitate proper derivatization and the use of chiral gas chromatography (GC) methods, which can be time-consuming. These limitations hinder the application of chromatography for high-throughput analysis, an increasingly important aspect due to the widespread adoption of automation techniques.

Nuclear magnetic resonance (NMR) presents an alternative approach for enantioanalysis.[7] This is typically achieved through the formation of diastereoisomeric species, which exhibit distinct spectroscopic signatures. Recently, there has been increasing interest in the unique capabilities of ^{19}F NMR for use in enantioanalysis.[8] The rarity of organofluorine compounds in nature, combined with the 100% natural abundance of the ^{19}F nucleus, makes ^{19}F NMR a preferred choice for analytical techniques due to its low background interference and high sensitivity. Furthermore, the high sensitivity of ^{19}F NMR chemical shifts to changes in the local environment makes it suitable for discriminating spectroscopic differences caused by stereoconfiguration. Various ^{19}F-labeled chiral derivatizing agents have been developed, facilitating the chiral discrimination of a wide range of analytes containing amino or hydroxy groups.[9] As an alternative to covalent derivatization, ^{19}F-labeled probes capable of reversibly binding to the analyte have been explored. When the chemical exchange rate is slow on the NMR timescale, distinct ^{19}F NMR signals corresponding to each enantiomer are produced.[10] This approach combines the benefits of operational simplicity and ease of spectrum interpretation, which is often referred to as recognition-enabled chromatographic ^{19}F NMR.[11] Although this method has been applied to the detection of various chiral substances, demonstrating a broader scope than derivatization-based methods, few investigations have focused on strategies to tune the resolving ability of the ^{19}F-labeled probe. Previously, we demonstrated that altering the metal center and constructing Lewis acid–base pairs can enhance the performance of chiral discrimination systems.[12] In this report, we present that adjusting the torsion angle is an effective strategy to improve the resolving ability. Compared to the CF_3-labeled cyclopalladium

[a] *The Education Ministry Key Lab of Resource Chemistry and Shanghai Key Laboratory of Rare Earth Functional Materials, Shanghai Normal University, Shanghai 200234, China*
[b] *Key Laboratory of Fluorine and Nitrogen Chemistry and Advanced Materials, Shanghai Institute of Organic Chemistry, University of Chinese Academy of Sciences, Chinese Academy of Sciences, 345 Ling-Ling Road, Shanghai 200032, China. E-mail: zhaoyanchuan@sioc.ac.cn*
[c] *Instrumental Analysis Center, Shanghai Institute of Organic Chemistry, Chinese Academy of Sciences, Shanghai, 200032, China*

† Electronic supplementary information (ESI) available. See DOI: https://doi.org/10.1039/d4cc01313a

‡ These authors contributed equally to this work.

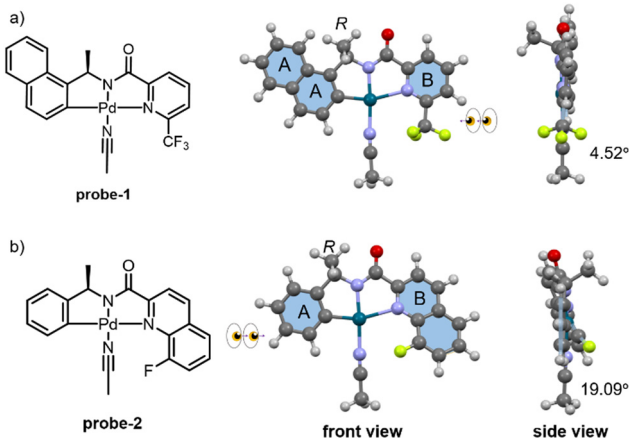

Scheme 1 DFT calculation of **probe-2** and **probe-1**.

probes developed earlier,[13] the new probe is characterized by a larger torsion angle, due to steric repulsion between the fluorine atom and the bound analyte (Scheme 1). This significant twisting of the probe's backbone leads to superior resolving ability in the chiral discrimination of amines, amino acid esters, nitriles, and N-heterocycles.

Recently, we developed ^{19}F-labeled cyclopalladium complexes for the enantiodifferentiation of N-heterocycles and nitriles. These complexes have shown that a methyl-substituted chiral center can cause the probe's backbone to twist, indicating a transfer from point chirality to helical-like chirality.[13] We hypothesize that this asymmetric backbone is critical for enantioresolution, as evidenced by the distinct ^{19}F NMR chemical shift differences corresponding to the enantiomers. If this hypothesis is correct, adjusting the twist of the probe's backbone could be an effective method for controlling the enantiodifferentiation performance of ^{19}F-labeled probes. With this approach, we initiated our research by synthesizing a fluorinated quinoline-based ligand, replacing the previously used pyridine-containing ligand (Scheme 1(a)). This new design ensures that the fluorine atom's position in the probe is static, unlike the mobile ^{19}F atom in the CF_3 group. The stationary ^{19}F atom is expected to experience increased steric repulsion with bound acetonitrile or analytes, resulting in a significant torsion angle (Scheme 1(b)). This alteration will move the probe's backbone away from a planar structure, potentially enhancing its chiral discrimination capability. To assess whether our design would result in the anticipated increased twisting of the probe's backbone, we conducted density functional theory (DFT) calculations on the optimized structures of both the previously reported **probe-1** and the newly designed **probe-2**. Our computations revealed a significant change in the torsion angle due to the replacement of the pyridyl group with quinoline (Fig. S21 in ESI†). Specifically, for **probe-2**, complexation with acetonitrile led to a substantial torsional angle of 19.09°, a notable increase compared to the 4.52° observed in **probe-1** (Scheme 1). Building on these insights, we proceeded to synthesize the targeted ^{19}F-labeled **probe-2**. The synthesis began with readily available 8-fluoroquinoline-2-carboxylic acid (**3**). Converting acid **3** into its acid chloride with $SOCl_2$, we then reacted it with (*R*)-1-phenylethylamine to yield the desired **ligand-4**. A C–H palladation reaction was efficiently performed in acetonitrile at 80 °C, producing the designed **probe-2** in a high yield (Fig. S1 in ESI†). It is noteworthy that **probe-2** was isolated with a bound acetonitrile molecule, which can be substituted by various analytes. This dynamic ligand exchange property is pivotal to our chiral discrimination strategy, allowing for immediate detection following the mixing of the probe with an analyte. Having successfully synthesized **probe-2**, we conducted a comparative study to evaluate the enantiodifferentiation performance of **probe-1** and **probe-2**. Chiral discrimination experiments were conducted by combining ^{19}F-labeled probes with various analytes in $CDCl_3$, followed by the acquisition of the ^{19}F NMR spectra. To evaluate the probe's chiral discrimination capability, we employed a parameter known as "Resolution (R_s)".[14] Our analysis revealed that **probe-2** outperforms **probe-1** in the chiral discrimination of various analytes, as indicated by higher R_s values, shown in Fig. 1. For example, **probe-2** effectively differentiates chiral nitriles with distant chiral centers, in contrast to the inadequate enantiodifferentiation of $\mathbf{A_1}$ and $\mathbf{A_2}$ by **probe-1**. Moreover, **probe-2** showed enhanced discrimination for nitrile compounds with quaternary chiral centers and axial chirality (Fig. 1(c) and (e)). Notably, improved resolution with **probe-2** was also observed in the enantioanalysis of other nitriles, where well-separated ^{19}F NMR signals were evident, unlike the crowded signals seen with **probe-1** (Fig. 1(d), (f) and (g)). Besides nitrile compounds, **probe-2** also demonstrated superior discrimination of amines with β-chirality centers (Fig. 1(h) and (i)). These observations suggest that **probe-2** is more sensitive to stereoconfigurations distal from the palladium metal, a feature difficult for **probe-1** to discern. Remarkably, aliphatic amines with substituents at the chirality center differing by just one methylene unit could be resolved by **probe-2**, a task known to be challenging for chiral HPLC. Consistent with our expectations, we observed a gradual decrease in the R_s values for analytes ranging from $\mathbf{A_{10}}$ to $\mathbf{A_{13}}$. This trend can be attributed to the increasing similarity in the size of the alkyl chains attached to the chiral carbon in these analytes. As the structural differences between the alkyl chains become less pronounced, the ability of the probe to differentiate between the enantiomers correspondingly diminishes, resulting in lower resolution values. For analytes already distinguishable by **probe-1**, a significant improvement in resolution was noted, with the R_s values increasing by factors of 3.2 to 9.9. This substantial enhancement in resolution augments the capability of this approach to analyze mixtures of structurally similar analytes in complex matrices (Fig. S2 in ESI†). It is important to note that for some analytes, such as $\mathbf{A_{19}}$, comparable spectral separation was observed between **probe-1** and **probe-2**. This could be attributed to the phenyl group in the analytes, where its shielding effect may significantly influence the overall spectral separation of the ^{19}F signal. These findings suggest that the augmented torsion angle leads to a structure that is less planar and more three-dimensional, enhancing the probe's ability to interact with and distinguish between the chiral centers of analytes more effectively. In an effort to amplify this structural twisting, we explored synthesizing a trifluoromethyl-substituted version of **probe-2**. However, the attempted C–H palladation reaction was

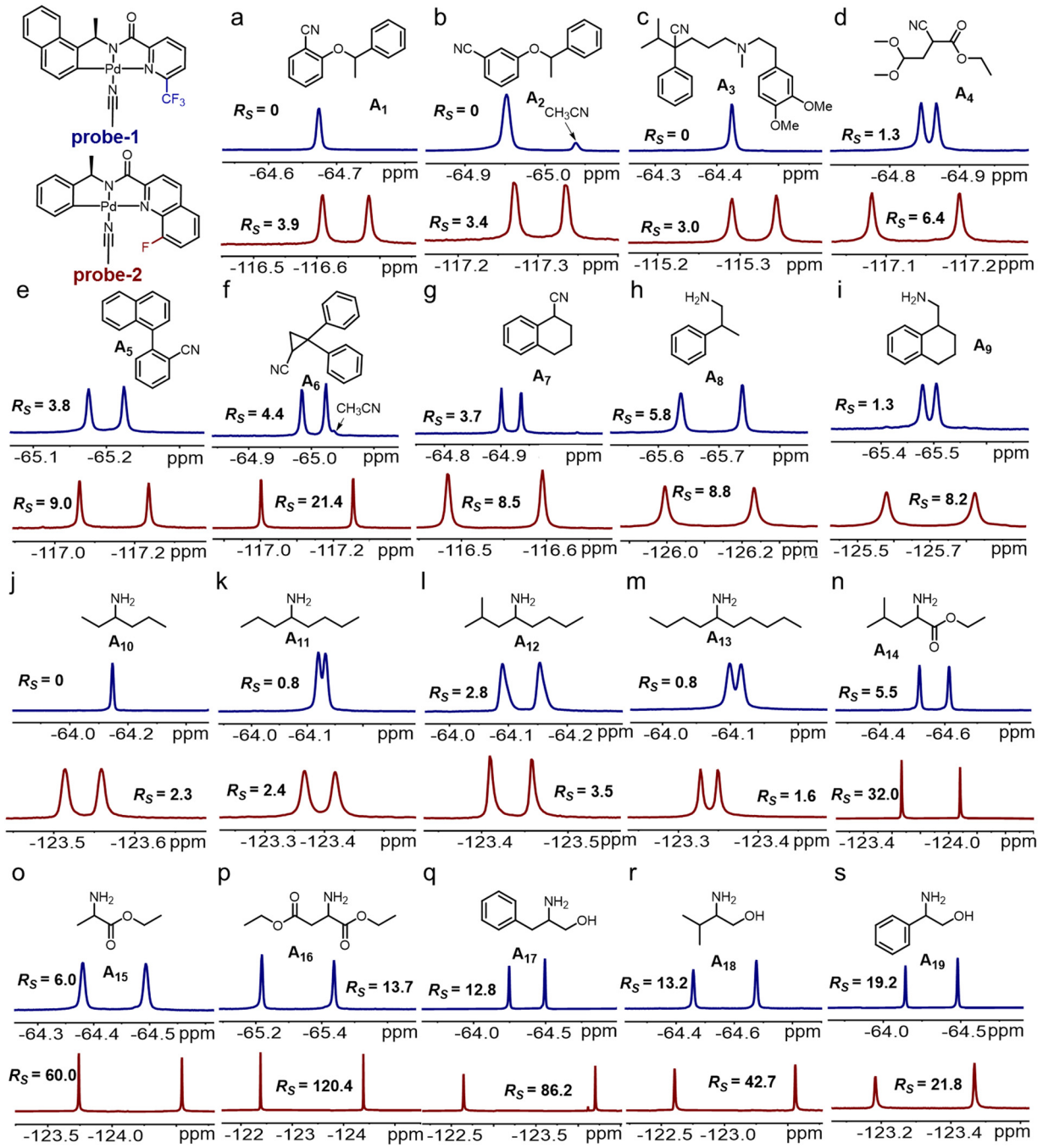

Fig. 1 (a)–(s) ^{19}F NMR spectra of mixtures containing ^{19}F-labeled probes and various analytes dissolved in deuterated chloroform ($CDCl_3$). The spectra associated with **probe-1** are presented in deep blue, while those corresponding to **probe-2** are depicted in dark red. All ^{19}F NMR measurements were conducted using a Bruker Avance Neo 600 MHz (565 MHz for the ^{19}F nucleus) NMR spectrometer, with each spectrum obtained from 64 scans. For the dark red spectra related to **probe-2**, ^{1}H-decoupled ^{19}F NMR techniques were employed.

unsuccessful. This failure could be attributed to increased steric repulsion between the bound acetonitrile molecule and the CF_3 group in the event that the palladium complex did indeed form. Such steric hindrance is likely a key factor impeding the reaction, rendering the formation of the complex energetically less favorable. In addition, we included an analysis comparing the performance of **probe-2** with another probe, similarly labeled with a ^{19}F atom but featuring a more planar backbone. The findings indicated that the probe with the planar backbone exhibited inferior performance relative to **probe-2** (Fig. S20 in ESI†). This suggests that the improved performance is not solely reliant on the replacement of the CF_3 label by a ^{19}F atom. To evaluate the effectiveness of **probe-2** in measuring the enantiomeric excess (ee) values of the enantioenriched samples, we employed $\mathbf{A_7}$ as a model analyte. When analyzing the racemic mixture, we noted that the ^{19}F NMR signal peak areas for both enantiomers were

identical (Fig. S3 in ESI†), indicating that **probe-2** has an equal affinity for $\mathbf{A_7}$ enantiomers with different stereoconfigurations. This characteristic enables the calculation of the ee values by directly comparing the peak areas of the ^{19}F NMR signals. Using this method, we observed a strong linear correlation between the calculated ee values and those determined by chiral HPLC analysis, validating the accuracy of our approach (Fig. S4 in ESI†). It's important to mention that for analytes where enantiomers exhibit different binding strengths towards the ^{19}F-labeled probe, a correction coefficient can be applied to account for the unequal binding affinity.[11,12] Our previous studies have shown that incorporating this correction coefficient allows for accurate determination of the enantiocomposition. The results achieved with this adjusted method showed an average absolute deviation of less than 2% compared to HPLC analysis, underscoring the reliability of this approach in enantiomeric analysis.

To demonstrate the capability of **probe-2** for quickly determining the enantioselectivity of transition-metal catalyzed reactions during the screening conditions, we chose a copper-catalyzed decarboxylative cyanation of benzyl acids as a model reaction. In this reaction, a complex of $Cu(acac)_2$ and bis(oxazoline)-type ligands acts as the catalyst, promoting enantioselectivity.[15] Trimethylsilyl cyanide and hypervalent iodine compounds are utilized as the cyanide source and oxidant, respectively. Previous studies have indicated that the enantioselectivity of this reaction is affected by both the ligand structure and the solvent used. We employed our method to rapidly determine the enantiomeric excess (ee) values of the products from the reaction under two different sets of conditions. For analysis, approximately 0.5 mL of the reaction mixture was sampled. The reaction was quenched with water, followed by extraction using ethyl acetate. After evaporating the organic phase under vacuum, the crude product was directly mixed with **probe-2** for ^{19}F NMR analysis. As shown in Fig. S16 (ESI†), our method yielded ee values of 83.8% and 80.8% for reactions conducted under conditions 1 and 2, respectively. These findings are in alignment with the values obtained through chiral HPLC analysis, which were 84.9% and 81.5%. It is noteworthy that bis(oxazoline)-type ligands produce ^{19}F NMR signals characterized by chemical shifts that differ from those produced by the nitrile products, thereby not affecting the ee assessments (Fig. S19 in ESI†). Typically, HPLC analysis requires a prepurification step, but our approach circumvents this necessity, demonstrating a significant advantage for high-throughput analysis. This method's ability to bypass extensive purification steps not only saves time but also makes it an attractive option for rapidly assessing the enantioselectivity of reactions in a more efficient manner.

In conclusion, we have developed a novel approach to enhance the resolving ability of chiral ^{19}F-labeled probes by manipulating the structural twisting of the probe's backbone. It is demonstrated that strategically replacing the pyridyl moiety with a 2-fluoroquinolyl group leads to a significant torsion angle. This structural alteration increases the probe's sensitivity to discern both distal chiral centers and chiral centers substituted by very similar alkyl groups. Enhanced chiral resolving capabilities were observed across a range of chiral analytes, including nitriles, amines, and amino alcohols. Computational simulations have provided further insights into how this modification induces structural twisting. We anticipate that this new strategy will extend to the design of other chiral probes, beyond those based solely on NMR techniques. The advancement in ^{19}F-labeled chiral probes is expected to significantly expedite progress in related fields, particularly asymmetric catalysis and drug discovery.

This work was supported by the National Natural Science Foundation of China (22271305) and the Strategic Priority Research Program of the Chinese Academy of Sciences (XDB0590000).

Conflicts of interest

There are no conflicts to declare.

Notes and references

1 (*a*) K. Bingol, L. Bruschweiler-Li, D. Li, B. Zhang, M. Xie and R. Brüschweiler, *Bioanalysis*, 2016, **8**, 557; (*b*) J. Du, M. Hu, J. Fan and X. Peng, *Chem. Soc. Rev.*, 2012, **41**, 4511; (*c*) M. A. De La Fuente and M. Juárez, *Crit. Rev. Food Sci. Nutr.*, 2005, **45**, 563; (*d*) L. Vaclavik, A. Schreiber, O. Lacina, T. Cajka and J. Hajslova, *Metabolomics*, 2012, **8**, 793; (*e*) D. R. Milićević, M. Škrinjar and T. Baltić, *Toxins*, 2010, **2**, 572; (*f*) C. K. Ho, A. Robinson, D. R. Miller and M. J. Davis, *Sensors*, 2005, **5**, 4; (*g*) J. Jiang, L. Wen, H. Wang, X. Chen, Y. Zhao and X. Wang, *J. Fluorine Chem.*, 2023, **226**, 110085.
2 (*a*) X. Wu, Z. Li, X. X. Chen, J. S. Fossey, T. D. James and Y. B. Jiang, *Chem. Soc. Rev.*, 2013, **42**, 8032; (*b*) O. R. Miranda, B. Creran and V. M. Rotello, *Curr. Opin. Chem. Biol.*, 2010, **14**, 728; (*c*) K. L. Diehl and E. V. Anslyn, *Chem. Soc. Rev.*, 2013, **42**, 8596.
3 (*a*) L. D. Barron, *Chem. Soc. Rev.*, 1986, **15**, 189; (*b*) P. Cintas, *Angew. Chem., Int. Ed.*, 2002, **41**, 1139; (*c*) S. Yu and L. Pu, *J. Am. Chem. Soc.*, 2010, **132**, 17698; (*d*) L. Zhu and E. V. Anslyn, *J. Am. Chem. Soc.*, 2004, **126**, 3676.
4 (*a*) B. Kasprzyk-Hordern, *Chem. Soc. Rev.*, 2010, **39**, 4466; (*b*) K. H. Engel, *J. Agric. Food Chem.*, 2020, **68**, 10265.
5 (*a*) M. Liu, L. Zhang and T. Wang, *Chem. Rev.*, 2015, **115**, 7304; (*b*) F. Yang, M. Wang, D. Zhang, J. Yang, M. Zheng and Y. Li, *Chem. Rev.*, 2020, **120**, 2693.
6 (*a*) P. Parrilla Vázquez, C. Ferrer, M. J. Martínez Bueno and A. R. Fernández-Alba, *TrAC, Trends Anal. Chem.*, 2019, **115**, 13; (*b*) W. H. Pirkle and T. C. Pochapsky, *Chem. Rev.*, 1989, **89**, 347; (*c*) Y. Okamoto and T. Ikai, *Chem. Soc. Rev.*, 2008, **37**, 2593; (*d*) J. Shen and Y. Okamoto, *Chem. Rev.*, 2016, **116**, 1094.
7 (*a*) H. Qian, M. Zhu, C. Gayathri, R. R. Gil and R. Jin, *ACS Nano*, 2011, **5**, 8935; (*b*) X. Li, K. H. Hopmann, J. Hudecová, J. Isaksson, J. Novotná, W. Stensen, V. Andrushchenko, M. Urbanová, J. S. Svendsen, P. Bouř and K. Ruud, *J. Phys. Chem. A*, 2013, **117**, 1721; (*c*) S. Immel, M. Köck and M. Reggelin, *J. Am. Chem. Soc.*, 2022, **144**, 6830.
8 (*a*) Z. Xu and Y. Zhao, *J. Fluorine Chem.*, 2023, **266**, 110089; (*b*) Z. Xu, C. Liu, S. Zhao, S. Chen and Y. Zhao, *Chem. Rev.*, 2019, **119**, 195; (*c*) H. Chen, S. Viel, F. Ziarelli and L. Peng, *Chem. Soc. Rev.*, 2013, **42**, 7971.
9 (*a*) M. Kriegelstein, D. Profous, A. Lyčka, Z. Trávníček, A. Přibylka, T. Volná, S. Benická and P. Cankař, *J. Org. Chem.*, 2019, **84**, 11911; (*b*) B. Huang, L. Xu, N. Wang, J. Ying, Y. Zhao and S. Huang, *Anal. Chem.*, 2022, **94**, 1867; (*c*) L. Xu, B. Huang, Z. Hou, S. Huang and Y. Zhao, *Anal. Chem.*, 2023, **95**, 3012.
10 (*a*) Y. Jia, L. Wen, W. Bao, Z. Xu, J. Wu and Y. Zhao, *Anal. Chem.*, 2023, **95**, 10362; (*b*) W. Wang, X. Xia, G. Bian and L. Song, *Chem. Commun.*, 2019, **55**, 6098.
11 (*a*) Y. Li, L. Wen, H. Meng, J. Lv, G. Luo and Y. Zhao, *Cell Rep. Phys. Sci.*, 2020, **1**, 100100; (*b*) Z. Xu and Y. Zhao, *Chem. Rec.*, 2023, e202300031.
12 (*a*) J. Liang, Z. Xu, J. Wu and Y. Zhao, *Anal. Chem.*, 2023, **95**, 7569; (*b*) H. Li, Z. Xu, S. Zhang, Y. Jia and Y. Zhao, *Anal. Chem.*, 2022, **94**, 2023.
13 (*a*) G. Gu, Z. Xu, L. Wen, J. Liang, C. Wang, X. Wan and Y. Zhao, *JACS Au*, 2023, **3**, 1348; (*b*) G. Gu, Y. Yue, C. Wang, W. Zhang, J. Wu, Y. Li and Y. Zhao, *Org. Lett.*, 2023, **25**, 4819.
14 C. Dong, Z. Xu, L. Wen, S. He, J. Wu, Q. H. Deng and Y. Zhao, *Anal. Chem.*, 2021, **93**, 2968.
15 Z. Li, G. Zhang, Y. Song, M. Li, Z. Li, W. Ding and J. Wu, *Org. Lett.*, 2023, **25**, 3023.